Photoreceptor Manifestations of Primary Mitochondrial Optic Nerve Disorders

Yin-Hsi Chang,[1,2] Eugene Yu-Chuan Kang,[1–3] Pei-Kang Liu,[4–7] Sarah R. Levi,[7] Hung-Hsuan Wang,[7] Yun-Ju Tseng,[7] Go Hun Seo,[8] Hane Lee,[8] Lung-Kun Yeh,[1,2] Kuan-Jen Chen,[1,2] Wei-Chi Wu,[1,2] Chi-Chun Lai,[1,2,9] Laura Liu,[1,10] and Nan-Kai Wang[7]

[1]Department of Ophthalmology, Chang Gung Memorial Hospital, Linkou Medical Center, Taoyuan, Taiwan
[2]College of Medicine, Chang Gung University, Taoyuan, Taiwan
[3]Graduate Institute of Clinical Medical Sciences, College of Medicine, Chang Gung University, Taoyuan, Taiwan
[4]Department of Ophthalmology, Kaohsiung Medical University Hospital, Kaohsiung Medical University, Kaohsiung, Taiwan
[5]School of Medicine, College of Medicine, Kaohsiung Medical University, Kaohsiung, Taiwan
[6]Institute of Biomedical Sciences, National Sun Yat-sen University, Kaohsiung, Taiwan
[7]Department of Ophthalmology, Edward S. Harkness Eye Institute, Columbia University Irving Medical Center, Columbia University, New York, New York, United States
[8]Division of Medical Genetics, 3billion, Inc., Seoul, South Korea
[9]Department of Ophthalmology, Chang Gung Memorial Hospital, Keelung, Taiwan
[10]School of Traditional Chinese Medicine, Chang Gung University, Taoyuan, Taiwan

Correspondence: Laura Liu, Department of Ophthalmology, Chang Gung Memorial Hospital, No. 5, Fu-Hsing Street, Kuei Shan, Taoyuan 333, Taiwan; laurajl@gmail.com.
Nan-Kai Wang, Department of Ophthalmology, Edward S. Harkness Eye Institute, Columbia University Irving Medical Center, Columbia University, 635 West 165th Street, New York, NY 10032, USA; wang.nankai@gmail.com.

Received: December 24, 2021
Accepted: April 19, 2022
Published: May 4, 2022

Citation: Chang YH, Kang EYC, Liu PK, et al. Photoreceptor manifestations of primary mitochondrial optic nerve disorders. *Invest Ophthalmol Vis Sci.* 2022;63(5):5. https://doi.org/10.1167/iovs.63.5.5

Purpose. To compare the manifestations of photoreceptors (PRs) in three hereditary optic neuropathies affected by primary mitochondrial dysfunction and discuss whether the retinal ganglion cells (RGCs) or the PRs are preferentially affected.

Methods. A retrospective analysis of patients with genetically confirmed diagnoses of optic neuropathies associated with mitochondrial dysfunction was performed. This cohort included Leber's hereditary optic neuropathy (LHON), autosomal dominant optic atrophy type 1 (OPA1), and optic atrophy type 13 (OPA13). Patient chart evaluations included clinical characteristics, best-corrected visual acuity (BCVA), fundus photography, spectral-domain optical coherence tomography (SD-OCT), electroretinogram (ERG), and visual evoked potential data.

Results. This analysis included seven patients with LHON, six with OPA1, and one with OPA13 from a tertiary medical center. Thirteen of the 14 individuals were male. The average BCVA at diagnosis was 20/285 and 20/500 in the right and left eyes, respectively. Five of the seven patients with LHON, and three of the six patients with OPA1 also showed a mild amplitude reduction or delayed latency on light-adapted ERG and 30-Hz flicker responses; however, SD-OCT imaging did not show correlated PR abnormalities. Notably, a 7-year follow-up of a patient with OPA13 revealed degeneration of RGCs prior to the degeneration of PRs. Follow-up data also demonstrated continuous loss of cone outer segment tips on SD-OCT imaging.

Conclusions. RGCs are, in general, affected by mitochondrial dysfunction, whereas variable PR dysfunction exists in patients with LHON and OPA1, especially with respect to the cone responses. Involvement of PRs is particularly evident in OPA13 after RGC degenerations.

Keywords: cone, electroretinogram, leber's hereditary optic neuropathy, mitochondrial dysfunction, optic atrophy, retinal degeneration, SSBP1

Mitochondrial diseases are a group of clinically heterogeneous genetic disorders caused by mitochondrial dysfunction.[1] Mitochondria are known to be crucial in cellular metabolism. Given that the mitochondria are under the dual control of both nuclear and mitochondrial genomes, genetic defects in either genome may result in changes in mitochondrial structural proteins, subunits of the respiratory chain, translation factors, or proteins crucial for the maintenance of mitochondrial DNA (mtDNA).[2,3] Consequently, such mutations lead to downstream impairment of oxidative phosphorylation (OXPHOS), the process of adenosine triphosphate production, Krebs cycle and folate cycle deficits, lack of enzyme intermediates, and accumulation of toxic substances.[4,5]

In human eyes, the retina and neurons are among the most metabolically active tissue. Retinal ganglion cells (RGCs), for example, are rich in mitochondria and are particularly vulnerable to mitochondrial dysfunction.[6] In order to maintain normal signal transmission, RGCs require a healthy population of mitochondria with adequate biogenesis,

Copyright 2022 The Authors

This work is licensed under a Creative Commons Attribution-NonCommercial-NoDerivatives 4.0 International License.

Downloaded from iovs.arvojournals.org on 04/24/2024

transportation, and remodeling.[7] Furthermore, these mitochondria are highly dynamic—they are continuously changing their location, fusion, and fission in order to meet their energetic demand.[8]

Leber's hereditary optic neuropathy (LHON; MIM #535000) was the first identified human disease linked to a point mutation in mtDNA, mainly affecting complex I of the respiratory chain.[9,10] Clinically, LHON causes bilateral painless loss of central vision with subsequently optic nerve atrophy in young male adults. A small number of patients also had neurological deficits such as postural tremor, peripheral neuropathy, dystonia, or ataxia. Optic atrophy type 1 (OPA1; MIM #165500) is another inherited disease associated with mitochondrial dysfunction; it is characterized by bilateral progressive visual loss, color discrimination impairment, and optic disc pallor.[11] The nuclear gene *OPA1* encodes a dynamin-related GTPase that regulates mitochondrial fusion and cristae integrity.[12] Upon investigation of the underlying ocular pathology of LHON and OPA1, studies revealed that they are both caused by a primary loss of RGCs.[13]

Optic atrophy type 13 (OPA13; MIM #165510) was recently classified in a group of patients with apparently dominant optic atrophy and mutations in the nuclear-encoded mitochondrial single-strand binding protein 1 (*SSBP1*) gene.[14–16] Although patients with other optic neuropathies have photoreceptor (PR) layers that are generally well preserved, some patients with OPA13 present with pigmentary changes and foveopathies.[14,16] Its causative gene, *SSBP1*, is a housekeeping gene involved in mitochondrial biogenesis, including mtDNA replication, and maintenance of the genome stability as a single-stranded DNA–binding complex.[17,18] Although OPA13, LHON, and OPA1 are all associated with mitochondrial dysfunction, it remains unknown why PRs are more severely affected in OPA13, specifically.

RGCs and PRs are densely packed with mitochondria and consume substantial energy.[19] Most studies and clinical experiments have focused on the clinical manifestation and pathophysiology of RGC damage, whereas changes in PR function have seldom been investigated among these mitochondrial optic neuropathies. Within the literature, three reports have described potential cone dysfunction[20–22]; however, the extent, severity, and mechanism of cone dysfunction were neither specified further nor elucidated. Additionally, the literature lacks any comprehensive electrophysiological studies comparing the difference between mitochondrial diseases.

In the present study, we compare the PR manifestations across various mitochondrial diseases and discuss possible mechanisms to explain the variable PR degeneration in patients diagnosed with LHON, OPA1, or OPA13.

Methods

Patients

Retrospective chart review was performed of patients seen and evaluated at Chang Gung Memorial Hospital (CGMH) Medical Center (Linkou and Taipei branches). Clinical images and medical records were analyzed from patients with genetically confirmed diagnoses of LHON (P1–P7), OPA1 (P8–P13), and OPA13 (P14). Patient consent was obtained as detailed by the Institutional Review Board of Chang Gung Memorial Hospital–approved protocol (201601569B0C602), and all procedures were conducted in accordance with the tenets of the Declaration of Helsinki.

Ophthalmic Examination

Patients underwent a detailed ophthalmic examination that included best-corrected visual acuity (BCVA), intraocular pressure, fundus examination, color fundus photography, spectral-domain optical coherence tomography (SD-OCT), electroretinography (ERG), and visual evoked potential (VEP). Fundus photos were taken in a 45° × 45° field. A macular thickness map and retinal nerve fiber layer (RNFL) analysis were obtained through SD-OCT (Heidelberg Engineering, Heidelberg, Germany). The ERG was performed using Burian–Allen contact lens electrodes, according to International Society for Clinical Electrophysiology of Vision standards,[23] and the stimuli were recorded using either the Utas-E3000 system (LKC Technologies, Inc., Gaithersburg, MD, USA) at Taipei CGMH or the Diagnosys Espion system (Diagnosys LLC, Lowell, MA, USA) at Linkou CGMH.

Genetic Tests

DNA was extracted from peripheral blood using the QIAamp DNA Mini Kit (QIAGEN, Valencia, CA, USA), as previously described.[24] All DNA samples were analyzed using whole exome sequencing[25] and subsequently verified by Sanger sequencing of the mutations located in the *OPA1* and *SSBP1* genes. LHON diagnoses were confirmed by polymerase chain reaction using a MyCycler Thermal Cycler (Bio-Rad Laboratories, Hercules, CA, USA) and purification, followed by sequencing to confirm one of the three hotspots (m.11778G>A, m.14484T>C, or m.3460G>A).

Results

Demographic Data

The demographic information for all 14 patients is summarized in Table 1. Seven patients were diagnosed with LHON (P1–P7), six patients with OPA1 (P8–P13), and one patient with OPA13 (P14). Thirteen of the 14 patients were male. The only female patient was diagnosed with OPA1 (P8). The mean age at evaluation was 43.3 years for LHON, 21.8 years for OPA1, and 16 years for OPA13. All of the patients in this study were from Taiwan, but we could not associate a clinical presentation to a specific haplogroup nor contribute the severity of clinical phenotype to the diversity in our patients. Most of the patients presented with blurry or decreased central vision. For all patients, mean BCVA was approximately 20/285 in the right eye (OD) and 20/500 in the left eye (OS) at diagnosis. It was numerically better in the OPA1 group (OD, 20/77; OS, 20/45) compared to the LHON group (OD, 20/1000; OS, 20/666) or OPA13 (OD, 20/200; OS, 20/100). Overall, no patients in this study had any known systemic involvement.

Leber's Hereditary Optic Neuropathy

One of the seven LHON patients carried the homoplasmic m.14484T>C mutation, and the remaining six patients carried m.11778G>A mutations—five of which were homoplasmic (Supplementary Table S1). No other mutations were revealed in the seven patients by whole exome sequence. Among these patients, fundus photography revealed

Investigative Ophthalmology & Visual Science

Downloaded from iovs.arvojournals.org on 04/24/2024

Downloaded from iovs.arvojournals.org on 04/24/2024

Table 1. Clinical and Demographic Summary of Patients Diagnosed with Mitochondrial Disease

Diagnosis	Patient ID	Age at Onset/ Evaluation	Sex	Gene Variant	Amino Acid Variant	BCVA at Evaluation (OD, OS)	Optic Disc Pallor	RNFL Thickness at Last Follow-Up (OD/OS)				Foveopathy on OCT (OD/OS)	Foveal Thickness (OD/OS)
								Inferior	Superior	Nasal	Temporal		
LHON	P1	50/51	M	m.14484T>C	p.Met64Val	20/400, CF/90 cm	No	158/154	142/138	69/60	74/75	No/no	255/242
	P2	59/60	M	m.11778G>A	p.Arg340His	20/1000, 20/1000	Temporal	65/91	77/82	43/52	29/45	No/pucker	299/310*
	P3	13/34	M	m.11778G>A	p.Arg340His	CF/30 cm, CF/25 cm	Diffuse	48/42	44/52	21/22	26/27	No/no	293/276
	P4	15/16	M	m.11778G>A	p.Arg340His	20/500, 20/500	Temporal	106/79	138/116	50/25	53/37	No/no	296/269
	P5	40/41	M	m.11778G>A†	p.Arg340His	20/400, 20/130	No	134/125	133/123	84/66	66/84	No/no	239/231
	P6	34/54	M	m.11778G>A	p.Arg340His	20/500, 20/2000	Diffuse	112/59	92/81	46/35	27/25	Drusen/no	251/289
	P7	26/27	M	m.11778G>A	p.Arg340His	20/2000, 20/250	Diffuse	102/91	118/59	54/48	47/44	No/no	282/284
OPA1	P8	8/16	F	c.1732A>C	p.Thr578Pro	20/200, 20/100	Temporal	97/91	110/62	56/39	39/35	No/no	255/245
	P9	18/37	M	c.1230+2T>C	Splice donor	20/130, 20/100	Diffuse	83/82	93/107	48/45	30/30	No/no	249/254
	P10‡	10/17	M	c.1230+2T>C	Splice donor	20/50, 20/100	Diffuse	59/60	88/97	35/18	36/48	No/no	263/273
	P11	4/21	M	c.112C>T	p.Arg38Ter	20/65, 20/65	Temporal	97/92	102/114	68/59	35/34	No/no	236/233
	P12	NA/33	M	c.980G>A	p.Arg327Gln	20/100, 20/100	Temporal	122/118	133/130	59/54	29/32	No/no	279/263
	P13‡	NA/7	M	c.980G>A	p.Arg327Gln	20/22, 20/20	Temporal	86/82	99/96	47/40	32/33	No/no	229/235
OPA13	P14	8/16	M	SSBP1c.320G>A	p.Arg107Gln	20/200, 20/100	Diffuse	57/54	49/45	35/37	24/17	Yes/yes	241/245

M, male; F, female.

* This patient was not included in the analysis of foveal thickness due to trauma, with a history of vitrectomy in his left eye.

† P5 carried a heteroplasmic m.11778G>A mutation, whereas the other patients with LHON were homoplasmic.

‡ P10 was the son of P9, and P13 was the son of P12.

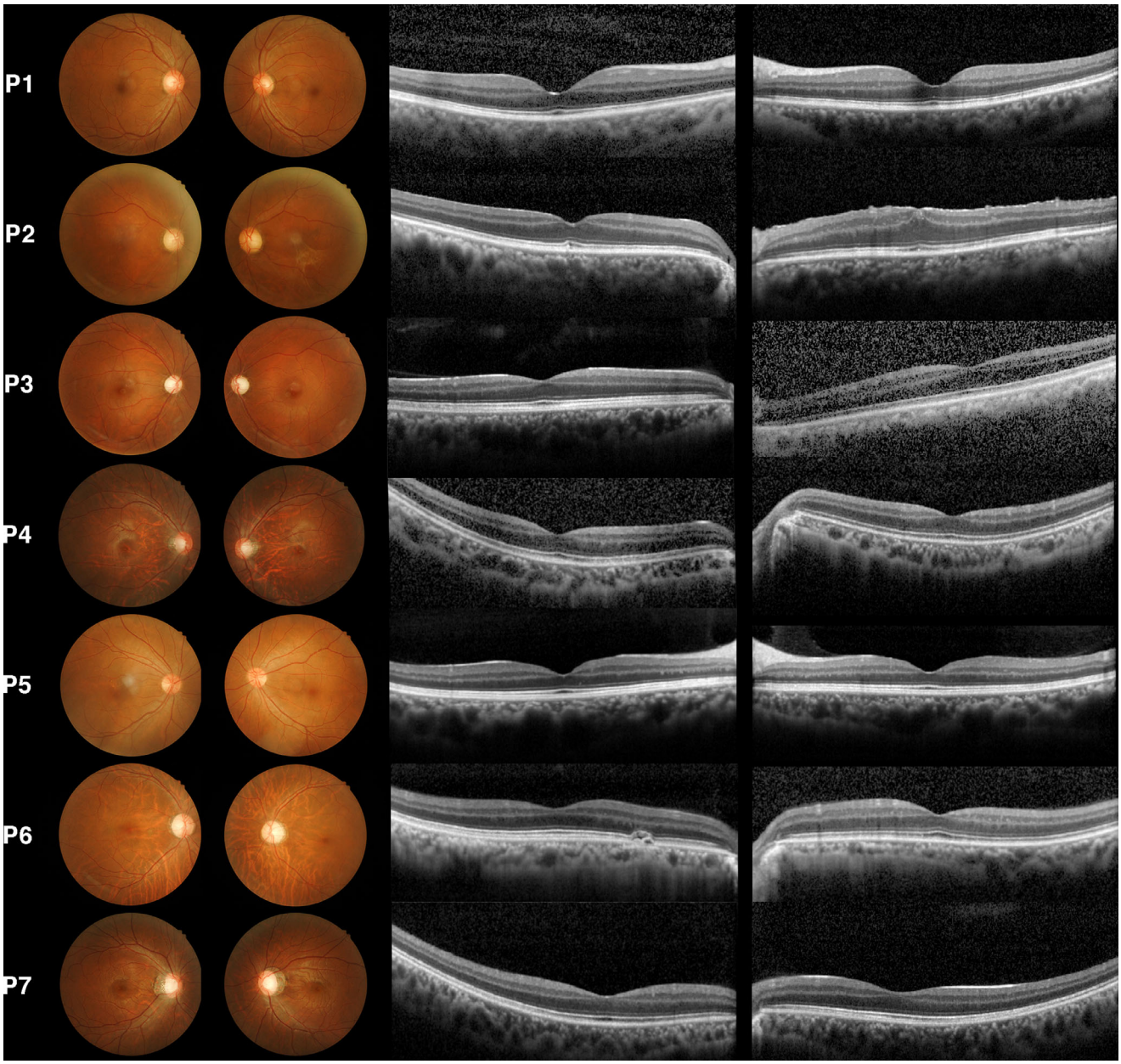

Figure 1. Color fundus photography and macula SD-OCT in patients with LHON (P1–P7). Optic disc pallor was present and symmetrical in both eyes of P1 to P4, P6, and P7. Among them, diffuse pallor is noticeable in P3, P6, and P7. Bilateral peripapillary atrophy can be seen in P4, P6, and P7. There were no vascular or pigmentary changes on fundus photography in any of the patients. Macular pucker can be seen in the left eye of P2 (who had a past medical history of trauma to the left eye) on both fundus photography and SD-OCT, leading to loss of normal foveal contour. P4 presented with a tessellated fundus related to his myopia (refractive error, –8 D; axial length, 27.5 mm). No other structural abnormalities were present in the other patients, except for P6, who had a small parafoveal drusen in the right eye on SD-OCT.

bilateral disc pallor, particularly affected in the temporal quadrant (Fig. 1). Three patients (P3, P6, and P7) carrying the m.11778G>A mutation had diffuse disc pallor. Overall, there were no obvious retinal pigmentary changes or vessel attenuation on the fundus photographs. On SD-OCT, a small parafoveal drusen was seen in the OD of P6. All other patients showed normal foveal contours (Fig. 1). Disc OCT of all subjects showed RNFL thinning, especially at the temporal side, correlated to the disc pallor (Fig. 2).

The full-field ERG results are summarized in Table 2. Four patients (P1, P4, P5, and P7) displayed a variable degree of decreased amplitude in dark-adapted b-wave and light-adapted 30-Hz flicker; four individuals (P1, P4, P6, and P7) had 30-Hz flicker implicit time delays over 30 ms; two patients (P4 and P5) also showed diminished b-wave amplitudes but no implicit time delay in the rod response. Both dark- and light-adapted ERGs were notably asymmetric in P4, who had glaucoma, whereas the other patients were symmetric. All patients had a decreased amplitude and delayed latency on pattern VEP, and some patients had a decreased amplitude on the N95 signal of their pattern ERG (Fig. 3), both indicating optic nerve dysfunction.

Investigative Ophthalmology & Visual Science

Downloaded from iovs.arvojournals.org on 04/24/2024

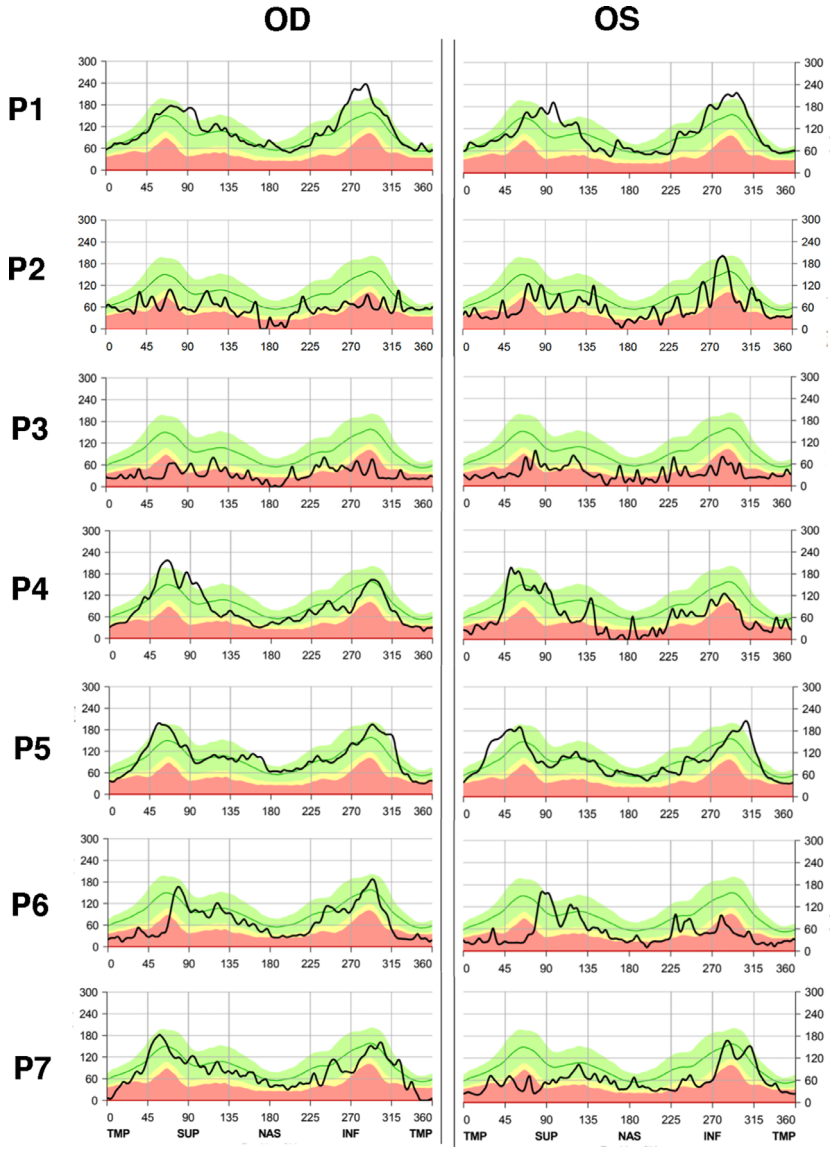

Figure 2. SD-OCT images of optic discs in patients with LHON (P1–P7). RNFL thickness was reduced in P1 to P4, P6, and P7, but P5 had mostly preserved RNFL thickness with focal thinning in the temporal quadrant in both eyes.

Optic Atrophy 1

Two father–son pairs (P9 and P10; P12 and P13) carried the point mutations c.1230+2T>C and c.980G>A in the *OPA1* gene, respectively. P9 and P10 had bilateral diffuse disc pallor, whereas the others had only temporal disc pallor (Fig. 4). No abnormal retinal pigmentary changes nor vessel structures were noted. SD-OCT imaging of the macula revealed intact external limiting membrane, ellipsoid zone (EZ), interdigitation zone (IZ), and retinal pigment epithelium (RPE) layers in all patients (Fig. 4). SD-OCT of the optic disc demonstrated RNFL thinning in the temporal region, whereas P8 and P11 also showed significant thinning in the nasal quadrant of the RNFL (Fig. 5).

In full-field ERG, tracings revealed a slight unilateral reduction in the amplitude of light-adapted 30-Hz flicker of P8 and P11, and a bilateral reduction in the amplitude of P13. A delay in 30-Hz flicker implicit time was present only in P8. Finally, the N95 signal on pattern ERG was significantly reduced in all patients, and pattern VEP showed an overall decrease in responses (Fig. 3).

Optic Atrophy 13

One case (P14), with a confirmed diagnosis of OPA13, revealed a mutation in the *SSBP1* gene at c.320G>A (p.Arg107Gln). This 16-year-old Taiwanese boy initially presented to the CGMH with poor vision, fair night vision, and color blindness in both eyes since childhood. His family history was unremarkable, and no consanguinity was reported. His BCVA was 20/100 OD and 20/200 OS at initial presentation. Fundus photography showed bilateral disc pallor and mild retinal vessel attenuation without obvious hyper- or hypo-autofluorescent change on fundus autofluorescence imaging (Fig. 6). SD-OCT of the macula showed thinning of the RNFL without other abnormality in the outer retina. Full-field ERG demonstrated decreased amplitude and delayed response of the b-wave for

Investigative Ophthalmology & Visual Science

Downloaded from iovs.arvojournals.org on 04/24/2024

Downloaded from iovs.arvojournals.org on 04/24/2024

Table 2. Full-Field Electroretinogram Findings of Patients Diagnosed with Mitochondrial Disease

		Dark-Adapted 0.01 ERG (OD/OS)		Dark-Adapted 3.0 ERG (OD/OS)		Light-Adapted ERG (OD/OS)			
Diagnosis	Patient ID	Amplitude (μV)	IT (ms)	a-Wave (μV)	b-Wave (μV)	a-Wave (μV)	b-Wave (μV)	30-Hz Flicker (μV)	30-Hz Flicker IT (ms)
LHON	P1	185.6/173.4	78/76	–167.3/–149.1	282.4/72.8	–32.3/–28.7	72.7/69.9	72.0/70.7	31.5/31
	P2	215.7/241.8	83/82	–175.6/–208.5	290.3/354.7	–31.2/–34.9	87.7/94.2	73.23/68.26	26/26
	P3	245.3/216.8	80/84	–199.9/–147.8	358.7/266.1	–39.3/–33.6	114.2/88.49	97.9/84.6	29/29
	P4	90.4/216.5	83.5/90	–58.4/–120.9	120.0/337.1	NA*/–20.9	NA*/64.3	21.9/43.4	30.5/31.5
	P5	130.1/131.1	84.5/82	–110.4/–131.5	207.8/218.6	–5.9/–38.4	43.2/50.2	56.5/56.5	29/29
	P6	267.9/284.1	84/90	–194.6/–207.9	369.7/373.3	–13.2/–20.6	86.8/105.6	65.1/72.8	31/29.5
	P7	343.5/218.4	91.5/106	–174.2/–108.1	430.6/401.8	–18.5/–19.4	79.2/61.4	65.4/49.1	31.5/32
OPA1	P8	272.7/256.6	83/84.5	–114.7/–90.8	456.3/419.1	–30.2/–53.9	95.95/103.8	61.8/77.4	30.5/30.5
	P9	192.8/148.6	85/104	–149.8/–136.5	276.2/225.8	–37.4/–22.6	94.1/72.3	84.0/78.1	28/28
	P10 (son of P9)	204.7/160.3	80/93	–153.5/–135.2	363.9/351.6	–25.5/–36.9	99.9/95.5	90.3/75.5	28/29
	P11	363.8/367.1	85/81.5	–149.8/–89.1	456.4/469.8	–29.5/–26.7	121.2/161.8	58.3/92.0	28/26.5
	P12	312.1/255.8	76/76	–228.9/–195.4	415.1/312.5	–41.7/–16.7	110/84.4	87.5/67.8	28.5/27.5
	P13 (son of P12)	325.2/198.8	100/78	–201.3/–187.8	381.0/332.5	–21.2/–33.7	55.1/82.8	35.3/36.7	29/28
OPA13	P14 (16 y)	146.4/128.5	98.5/96.5	–118.7/–104.7	185.6/161.2	–20.3/–16.2	60.1/67.2	59.6/73	29/28.5
	P14 (23 y)	56.7/54.4	80/85	–65.3/–52.8	94.0/70.0	–23.9/–21.5	47.6/43.9	50.4/36.1	29/29
Normal reference		218.5 ± 148.3	85.9 ± 14.1	−210.1 ± 172.1	347.0 ± 134.1	−36.4 ± 25.8	109.8 ± 67.8	121.4 ± 65.5	26.3 ± 3.8

IT, implicit time; NA, not available.
*Very low amplitude that was undetectable.

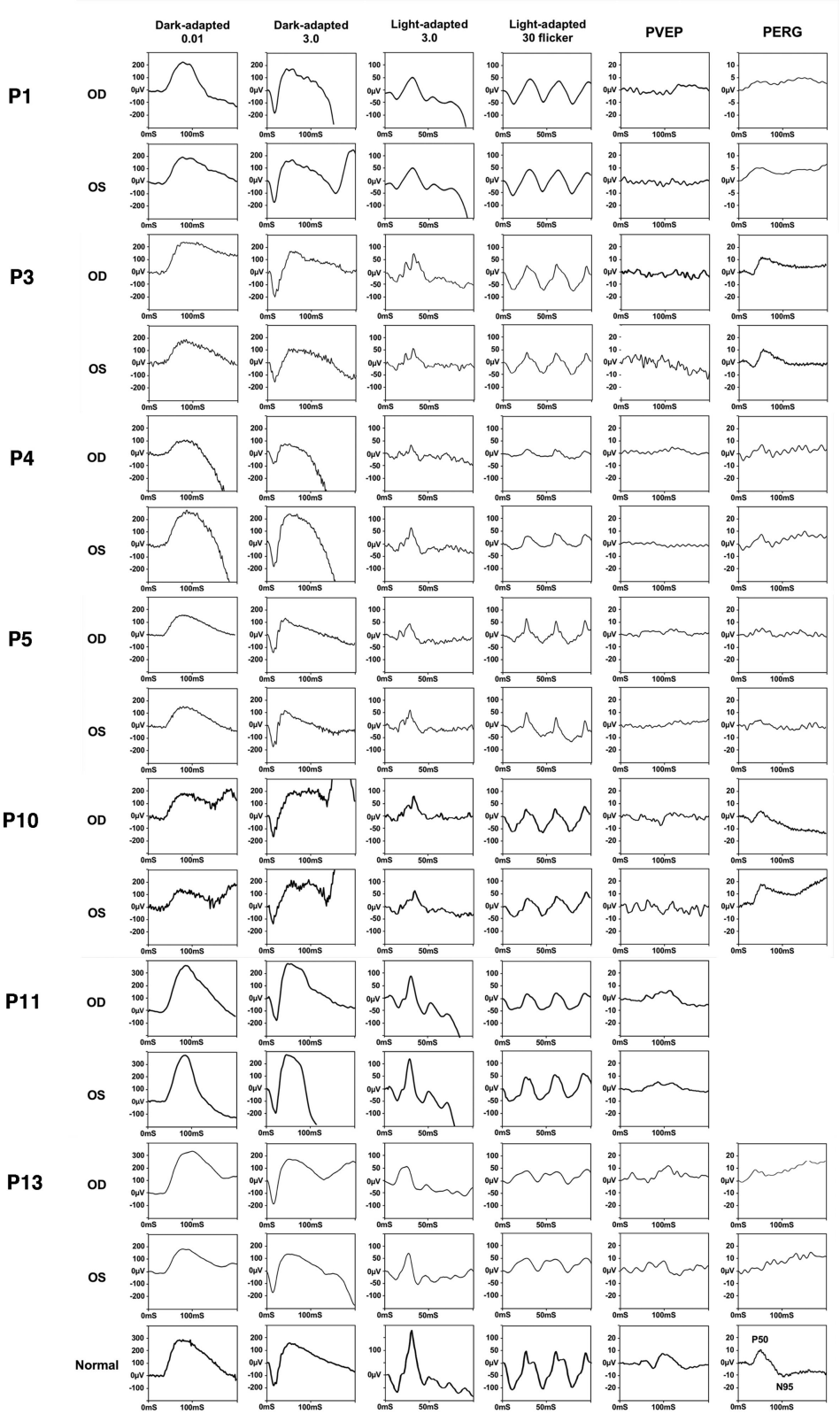

Figure 3. Electrophysiological studies in patients with LHON and OPA1. The full-field ERG study showed a reduced amplitude in the right eye of P4 and in bilateral eyes of P5 on dark-adapted ERG. A decreased amplitude was also seen in P1, P4, P5, and P13 (especially P4) on light-adapted ERG, and delayed implicit time was noted in P1 and P4 on 30-Hz flicker. Pattern VEP showed decreased responses in all individuals and was nearly extinguished in P4 and P5. The N95 signal on pattern ERG was reduced in all individuals with available pattern ERG.

Investigative Ophthalmology & Visual Science

Downloaded from iovs.arvojournals.org on 04/24/2024

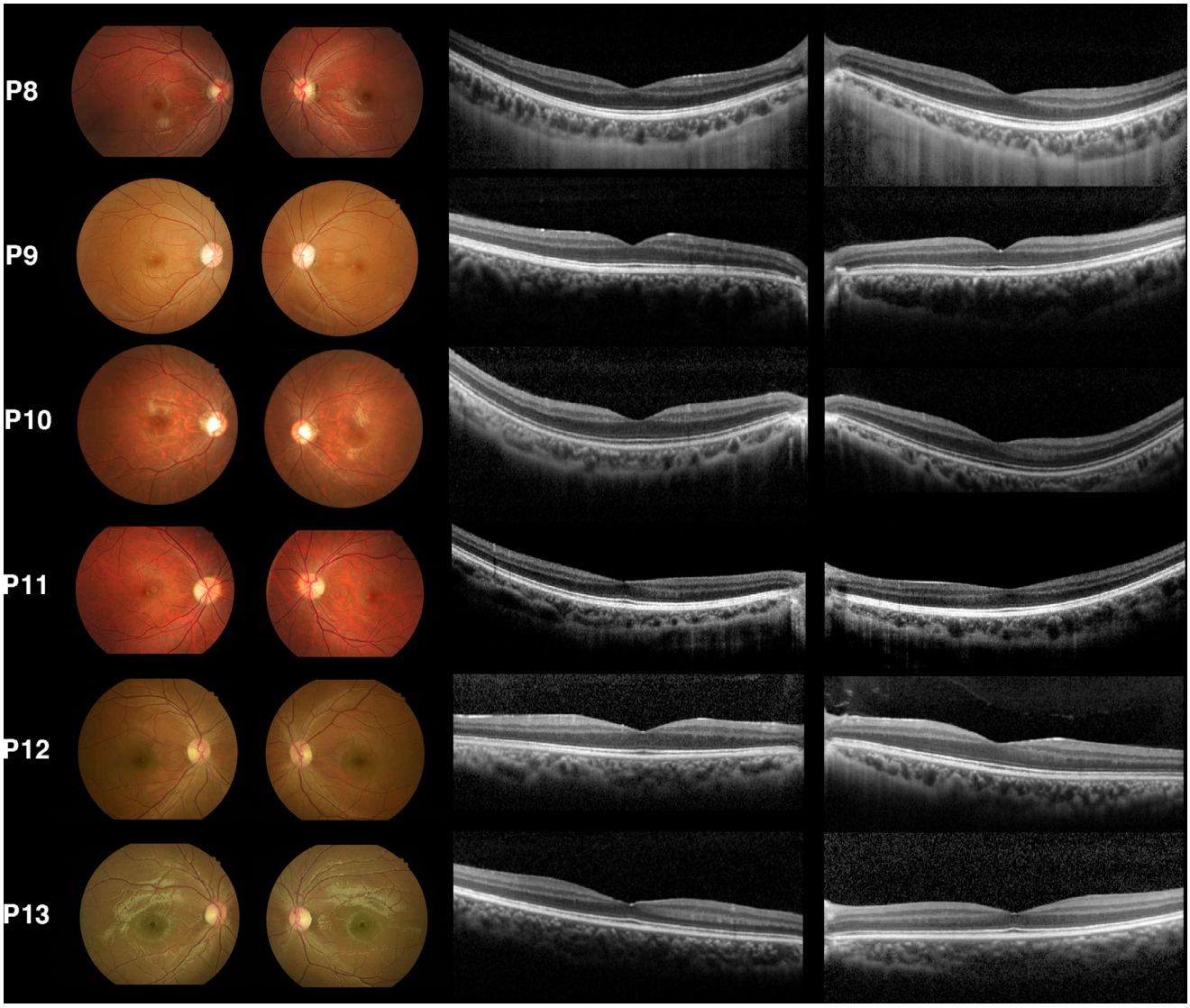

Figure 4. Color fundus photography and macula SD-OCT for patients with OPA1 (P8–P13). Optic disc pallor is shown in all affected individuals. P9 and P10 (father and son) both have particularly diffuse pallor. No other abnormality was observed on fundus photography or macular SD-OCT.

dark-adapted ERG; only a decreased amplitude was present in light-adapted ERG (Fig. 7). This finding is compatible with early stages of rod–cone degeneration. Finally, pattern VEP was extinguished. Taken together, P14 had more significant phenotypes of RGC dysfunction than PR degeneration at 16 years old.

The same patient (P14) underwent identical examinations 7 years later, at 23 years of age. His BCVA remained the same, but more significant disc pallor was noticed in both eyes (Fig. 6). Notably, the cone outer segment tip (COST) line diminished (Fig. 6, yellow arrowheads), visible as a foveal hyporeflective gap in the EZ and RPE. The full-field ERG showed progressively reduced amplitudes in both rod and cone responses compared to the tracings reported 7 years prior (Fig. 7). Although pattern VEP remained extinguished throughout the 7 years, pattern ERG N95 signal was almost undetectable in both eyes. Based on the progression data recorded, it can be concluded that this patient exhibited an optic atrophy combined with rod–cone degeneration.

Discussion

Conventionally, LHON and OPA share the same phenotype of RGC loss secondary to mitochondrial dysfunction. Here, we analyzed a cohort of patients with LHON, OPA1, and OPA13 and found that PR function was mildly affected in addition to RGC function in some cases of LHON and OPA1. More remarkably, this study revealed that combined RGC and PR death was noted in OPA13, distinguishing it from the other primary mitochondrial optic nerve disorders.

Photoreceptor Function in LHON

Typically, electrophysiological studies in LHON demonstrate normal full-field ERGs and abnormal flash VEP, pattern VEP, and pattern ERG responses, as expected in optic nerve disease. Although most patients displayed these expected functional responses, sporadic cases revealed full-field ERG changes that indicated partial PR impairment. An early

Investigative Ophthalmology & Visual Science

Downloaded from iovs.arvojournals.org on 04/24/2024

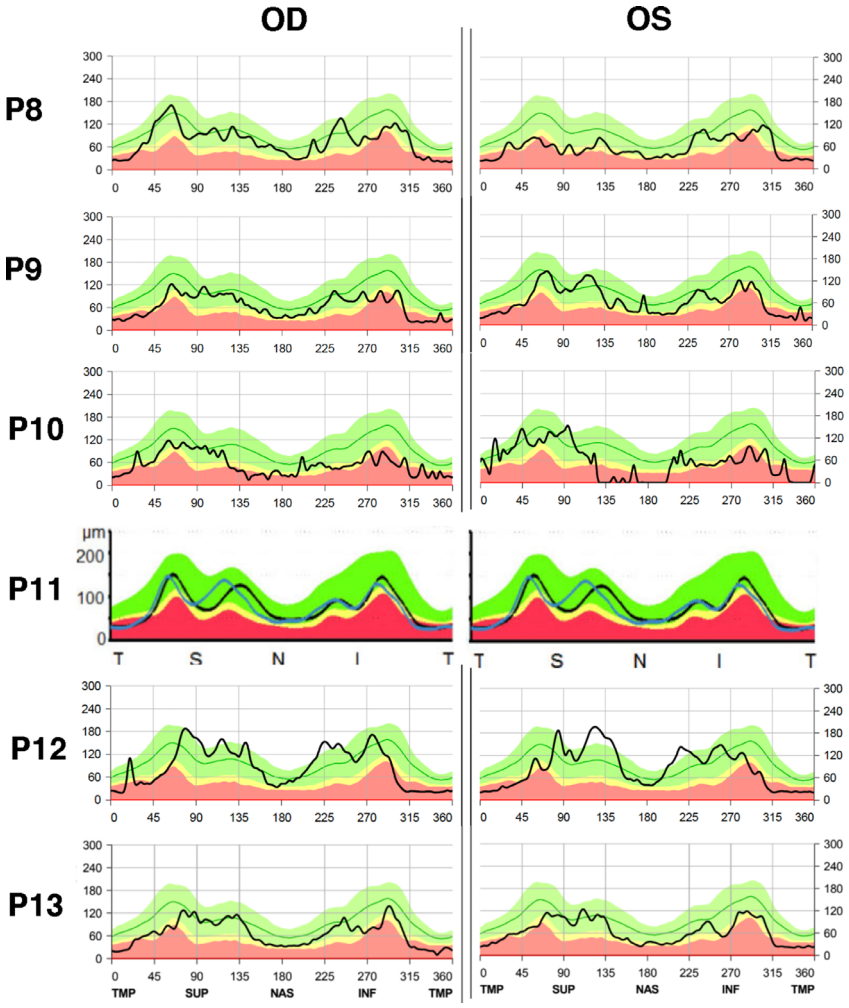

Figure 5. SD-OCT images of optic disc in patients with OPA1 (P8–P13). Diffuse thinning of the RNFL layer was seen in P8, P9, and P10; P11, P12, and P13 showed temporal thinning.

investigation of electrophysiological studies in 34 LHON patients reported that the general results were normal flash ERGs and abnormal flash and pattern VEPs; three individuals, however, presented with attenuation of b-wave on flash ERG.[20] In a Brazilian family all carrying the m.11778G>A homoplasmic mtDNA mutation, two of four members (mother and son) had abnormal full-field ERG responses.[21] The amplitudes for single-flash cone response and 30-Hz flicker were reduced, whereas the b-wave implicit times remained normal. In patients with certain mitochondrial disorders involving complex I, III, or IV, ERG findings revealed some abnormalities of the scotopic a-wave and postreceptoral b-wave.[26] In a mtDNA mutant mouse model, both scotopic and photopic responses showed a significant deficit with a reduction of 17% to 26% in the amplitudes of all ERG parameters.[27] Their tracings also displayed a trend toward increased latencies in the a- and b-waves. Similarly, our study revealed that five out of seven individuals had full-field ERG abnormalities. Of those five patients, two exhibited significantly reduced amplitudes in photopic response, as well as lower amplitudes in the scotopic response. Evidence from a previous study suggested that outer retinal layers on SD-OCT, such as the inner segment, outer segment, and RPE, did not have detectable structural changes in LHON subjects.[28] Similarly, in our investigation, SD-OCT imaging showed no obvious lesions. These findings suggest that LHON patients may have PR dysfunction in addition to RGC dysfunction, even in the absence of morphological presentation.

Photoreceptor Function in OPA1

For years, researchers and physicians have maintained that the disease hallmark of OPA1 is RGC degeneration with characteristically normal full-field ERG tracings.[29] In fact, a few analyses at a pre-ganglionic level have shown additional functional impairment in the retinal components. For example, Miyata et al.[30] examined the electrophysiological data of oscillatory potentials on full-field ERG and found the average amplitude of oscillatory potentials for eight OPA1 patients to be approximately half the average amplitude for the controls. Specifically, their findings revealed that the inner nuclear and plexiform layers, including the amacrine cells, may be defective in OPA1. Additionally, small, localized signals produced by multifocal ERG have provided additional evidence of pre-ganglionic retinal dysfunction in which the central amplitude reduction is observed.[31,32] Moreover, it has been reported that

Downloaded from iovs.arvojournals.org on 04/24/2024

Figure 6. Retinal images for P14, who has OPA13, at 16 and 23 years of age. When P14 was 16 years old, the color photography mosaic images showed bilateral optic disc pallor with a cup-to-disc ratio of 0.3 horizontally and vertically in both eyes. Additionally, loss of papillomacular bundles, retinal vessel attenuation, and some peripheral RPE depigmentation were noted. SD-OCT of the macula showed significant thinning of the ganglion cell layer and the axon toward the optic disc in the RNFL, mimicking a loss of foveal depression contour in both eyes. However, there was no foveopathy in terms of ellipsoid line loss or other abnormality in the outer retina. Autofluorescence imaging showed no obvious hyper-autofluorescent ring nor hypo-autofluorescent spots. At the 7-year follow-up visit, the disc pallor became more significant, and retinal vessel sheathing was present. Macula SD-OCT showed a loss of COST line (*yellow arrows*) at 23 years compared to that at 16 years.

the amplitude of maximal response and the single-flash photopic ERG in OPA1 patients were smaller than those in controls, although not reaching statistical significance.[30] These results were similar in a mouse model carrying a pathogenic mutation in *Opa1*.[33] In our study, we identified full-field ERG subnormalities, which mainly occurred in the photopic response. This susceptibility appeared to only affect PR physiological function as opposed to PR death, as seen on SD-OCT.[34,35] Nevertheless, the microstructure analyzed under three-dimensional electron microscopy

Investigative Ophthalmology & Visual Science

Downloaded from iovs.arvojournals.org on 04/24/2024

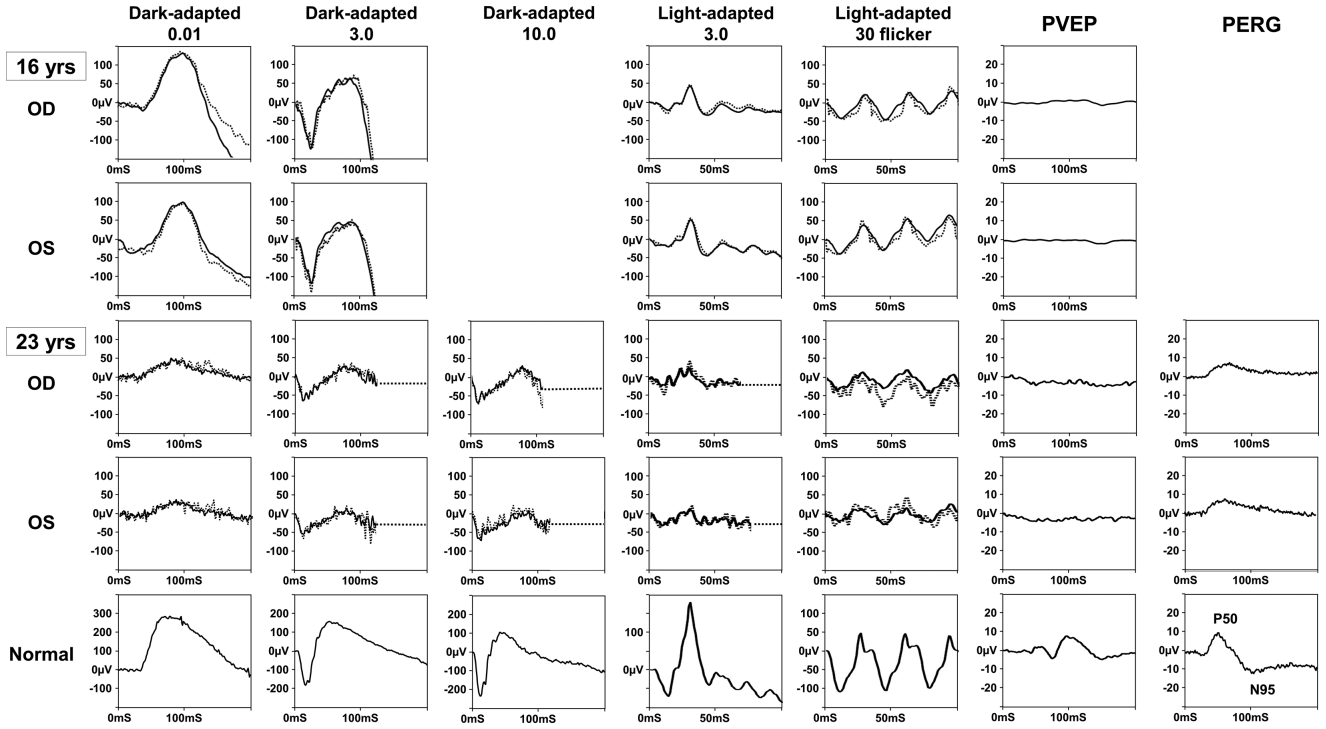

Figure 7. Electrophysiological studies of P14, who has OPA13, at 16 and 23 years of age. The full-field ERG revealed remarkably diminished amplitude on dark-adapted ERG and mildly reduced response on light-adapted ERG over a 7-year period (dash lines: right eye, solid lines: left eye). Pattern VEP remained the same at follow-up, maintaining almost no signal, whereas pattern ERG showed loss of the N95 component at the 7-year follow-up visit.

showed enlarged mitochondria with reduced alignment to neighboring mitochondria in the heterozygous *Opa1* knockout mouse.[36]

Susceptibility of RGCs Versus PRs

RGCs and PRs are both highly energy dependent, but RGCs are thought to be particularly susceptible in mitochondrial dysfunction such as LHON and OPA1, although these disorders present with far less frequent PR degeneration. Some metabolic differences between the two cell types may explain this phenomenon. First, PRs prefer aerobic glycolysis in the cytoplasm as their form of energy production. About 80% of the glucose supplied to the outer retina is metabolized by PRs into lactate via glycolysis.[37] PRs are assumed to be the primary site for aerobic glycolysis in the outer retina because they contain the glycolytic enzyme hexokinase, and in retinas that lack PRs the level of lactate is reduced.[38] By contrast, only 20% of glucose from the vascularized inner retina is converted to lactate, indicating that RGC dendrites are primarily reliant on OXPHOS in the mitochondria.[39] It may explain why mitochondrial dysfunction is more likely to cause RGC death, whereas PRs are able to maintain their function through glycolysis.

It is important to note that cones are more likely to be affected than rods in patients with LHON or OPA1. Previous studies demonstrating that PRs prefer glycolysis are mainly referring to rod cells, which account for 95% of PRs in mice and human.[40] It remains unknown whether cones also prefer glycolysis in the rod-dominant mammalian retina. Cones have been reported to contain twice as many mitochondria as rods in the mouse retina and 10 times as many in the primate retina.[41,42] In particular, a recent study using reporter mice showed that rods are more dependent on glycolysis than cones, which may imply that cones are more reliant on mitochondria as their energy source and therefore more susceptible to mitochondrial dysfunction than rods.[43] Taken together, we would expect more cone than rod dysfunction in patients with LHON or OPA1.

In addition to the preference of energy source, the second metabolic difference may lie with oxidative stress, which has long been believed to play a determining role in the pathophysiology of mitochondrial optic nerve diseases.[27] Normally, as the mitochondria metabolize oxygen, approximately 0.4% to 4% is not completely reduced through the electron transport chain, thereby becoming reactive oxygen species (ROS).[44] The cells have many defense mechanisms to counter the oxidative damage induced by ROS. Antioxidant enzymes, such as superoxide dismutase (SOD), catalase, and glutathione peroxidase, are the primary defense system in most cells.[45] However, lower levels of mitochondrial SOD were expressed in the optic nerve compared to other tissues, which reduced the protection against superoxide-related oxidative injury.[46,47] Specifically, OPA1 mutant cells exhibited a 3.4- to 4.2-fold increase in mitochondrial superoxide levels.[48] A certain toxic threshold may be reached in RGCs when ROS accumulation overwhelms the intrinsic antioxidant capacity, eventually leading to optic neuropathy. On the other hand, PRs are exposed to an oxygen-rich environment that may help them or adjacent RPE develop stronger antioxidativity. These differences can explain the increased vulnerability of RGCs to ROS damage compared with PRs.[49,50]

Third, RGCs may be more vulnerable than other cells due to their specialized structure.[51] The extremely long axons of

Investigative Ophthalmology & Visual Science

Downloaded from iovs.arvojournals.org on 04/24/2024

RBCs exit the eye to form the optic nerve and project along the visual pathway. Approximately 1 million axons per optic nerve are needed to transmit signals for 50-mm span from the retina to the brain.[52] Mitochondrial dysfunction could affect membrane dynamic equilibrium, cause energy deficiency, reduce mitochondrial mobility, or impede the efficacy of transportation.[12] In addition, the long axons are prone to axonal injury, leading to axonal degeneration.[53] A primary insult on an axon can increase superoxide expression in the soma and adjacent axons, mistakenly sending an apoptosis signal to RGCs.[54] Anatomically, PRs do not contain the axonal portion necessary for distal signal transduction; thus, PRs are less likely to be affected via axonal injury. This might explain why PR dysfunction is less common in patients with LHON or OPA1.

Evidence of Photoreceptor Degeneration in *SSBP1* Mutation

In contrast to LHON and OPA1, OPA13 mediated by *SSBP1* mutations is more likely to have photoreceptor degeneration in retinal images and electrophysiology. Four studies dating from 2019 to 2021 reported a total of 59 *SSBP1* mutant patients (Supplementary Table S2).[14–16,55] Among those 59 patients, 19 had available color fundus photography, revealing retinal vessel attenuation in 11 patients (57.9%), and pigmentary changes were seen in 12 patients (63.2%). Foveopathy, including focal disruption of the EZ and IZ bands, as well as complete or incomplete foveal cavitation, was shown on 26 of 44 macular SD-OCT scans (59.1%). Rod–cone degeneration was confirmed by full-field ERG in 11 of 40 individuals (27.5%). Interestingly, six of the 11 affected individuals (54.5%) carried the pathogenic variant c.320G>A, just as our patient P14 did, and three of 11 patients (27.3%) carried the c.113G>A variant. According to a study by Meunier et al.,[55] examining a large family, only two of 27 patients carrying the c.113G>A variant (7.4%) had confirmed rod–cone dystrophy and were possibly associated with greater age (mean, 69.5 years old) as compared to patients carrying the c.320G>A variant who presented with rod–cone dystrophy (mean, 37.2 years old). Both c.113G>A and c.320G>A are the two most common variants in the literature, and more patients with the c.320G>A compared to patients with the c.113G>A variant exhibit rod–cone degeneration. It is possible that PRs are relatively preserved in the c.113G>A variant, whereas PRs are more likely to be involved in the c.320G>A variant. Nevertheless, not every individual carrying the c.320G>A variant presents with retinal degeneration, indicating a variable expressivity for this gene.[55] Additional studies that include more patients with *SSBP1* variants are needed, in conjunction with complete retinal imaging, electroretinograms, and longer follow-ups, in order to better elucidate these findings.

It is likely that RGC death precedes PR degeneration in patients with *SSBP1* mutations.[15] In this study, the initial evaluation of P14 at age 16 years revealed apparent optic atrophy. At the 7-year follow-up, P14 showed remarkable attenuation of retinal vessels, loss of the COST line on SD-OCT, and generalized reduction of amplitude on full-field ERG. According to the literature, patients with retinal degeneration ranged in age from 17 to 54 years old at diagnosis, and the 54-year-old individual was reported to have the most severe rod–cone dysfunction, with almost undetectable waves on full-field ERG.[15] Another patient with longitudinal electrophysiological studies at 18 and 26 years old showed progressively worse rod–cone degeneration along with stationary RGC dysfunction over the 8-year period.[15] These findings support our hypothesis that RGCs are affected earlier than PRs and that PR function deteriorates with age. As for differences between cone and rod involvement in primary mitochondrial optic neuropathies, our ERG findings showed a more obvious decrease in rod signal compared to that of the cones, corroborated by Jurkute et al.[15] Additionally, we found diminished COST lines on SD-OCT in our patient (P14), which was not seen in any other patients with LHON or OPA1 within our cohort.

Function of SSBP1

The function of the mutated SSBP1 protein is not fully understood yet. Jurkute et al.[15] suggested that the product of the SSBP1 mutant function is a dominant-negative protein that may adversely interfere with SSBP1 wild-type activity. In their zebrafish experiment, three variants (c.113G>A, c.320G>A, and c.422G>A) showed a reduction in retinal *atoh7* expression in RGC precursors. Meanwhile, the dominant-negative effect is more commonly seen in multimeric enzymes, as in the case of SSBP1.[56] However, the dominant-negative effect did not present in the experiment by Del Dotto et al.[16] Their zebrafish model yields no apparent changes in the optic nerve phenotype of c.119G>T, c.184A>G, c.320G>A, c.331G>C, and c.394A>G variants, and even under the titration of wide-type and c.320G>A mRNA. Instead, functional null mutations were preferred. Future mouse models with mutations identified in our patient (c.320G>A) and the use of their tissue material for various genomic, transcriptomic, proteomic, and metabolomic analyses could uncover the pathophysiology associate with the c.320G>A variant.

The SSBP1 mutant appears to have the strongest evidence of outer retinal involvement compared to other primary mitochondrial optic neuropathies. This could be explained by the function of SSBP1, which is essential for DNA repair when mtDNA is damaged. It is easier to accumulate errors in mtDNA than in nuclear DNA because mitochondria lack essential repair pathways that the nucleus possesses, such as ribonucleotide excision repair and mismatch repair systems.[57] Various insults such as oxidation, radiation, environmental toxins, and intrinsic replication errors can result in damage. Mutations of SSBP1 can destabilize SSBP1 dimeric and tetrameric formation, leading to replicational dysfunction. Eventually, the cell is unable to maintain the minimal biophysiological requirement of mitochondrial function. Thus, a deficit in SSBP1 could affect numerous cells other than just RGCs. This mechanism could also explain the early onset of clinical symptoms in OPA13 compared to LHON and OPA1. Furthermore, the mitochondrial density is particularly high in PRs, which may allow for an increased tolerance of mitochondria "loss" than in RGCs.

Limitations

Within the constraints of this study, a few limitations are worth noting. First, given the low prevalence of mitochondrial diseases in the general population, we were only able to evaluate and compare a limited number of patients with confirmed diagnoses. In particular, we had only one patient with the *SSBP1* mutation. Second, in this case series we propose several explanations for how mitochondrial

Investigative Ophthalmology & Visual Science

Downloaded from iovs.arvojournals.org on 04/24/2024

dysfunction affects RGCs and PRs differently. Although this study provided comprehensive clinical data comparing patients with LHON or OPA1, as well as a close analysis of the sequential changes of PR function in a patient with OPA13, the precise mechanism of disease could not be confirmed due to limitations of our methodology. Moving forward, future studies will be necessary in order to validate the underlying pathophysiology leading to mitochondrial dysfunction.

Conclusions

In this study, a methodical analysis of 14 patients elucidated the fate of PRs resulting from primary mitochondrial optic neuropathies. Comprehensive evaluation of the data revealed subclinical PR degeneration in LHON and OPA1, whereas strong evidence of PR degeneration was shown in OPA13 mediated by a mutation in the *SSBP1* gene. It is likely that the phenotypes of OPA13 are the result of a mtDNA replication deficit that leads to the accumulation of intracellular damage, ultimately affecting both RGCs and PRs, sequentially.

Acknowledgments

Nan-Kai Wang and his lab are supported by the National Institute of Health R01EY031354, P30EY019007, P30CA013696, Vagelos College of Physicians & Surgeons (VP&S) Grants and Gerstner Philanthropies. Laura Liu and her lab are supported by a Chang Gung Memorial Hospital Research Grant CMRPG3M0631. The content is solely the responsibility of the authors and does not necessarily represent the official views of the National Institutes of Health.

Disclosure: **Y.-H. Chang**, None; **E.Y.-C. Kang**, None; **P.-K. Liu**, None; **S.R. Levi**, None; **H.-H. Wang**, None; **Y.-J. Tseng**, None; **G.H. Seo**, None; **H. Lee**, None; **L.-K. Yeh**, None; **K.-J. Chen**, None; **W.-C. Wu**, None; **C.-C. Lai**, None; **L. Liu**, None; **N.-K. Wang**, None

References

1. Gorman GS, Chinnery PF, DiMauro S, et al. Mitochondrial diseases. *Nat Rev Dis Primers*. 2016;2:16080.
2. Scarpulla RC. Transcriptional paradigms in mammalian mitochondrial biogenesis and function. *Physiol Rev*. 2008;88:611–638.
3. Calvo SE, Mootha VK. The mitochondrial proteome and human disease. *Annu Rev Genomics Hum Genet*. 2010;11:25–44.
4. DiMauro S, Schon EA. Mitochondrial respiratory-chain diseases. *New Engl J Med*. 2003;348:2656–2668.
5. Tuppen HAL, Blakely EL, Turnbull DM, Taylor RW. Mitochondrial DNA mutations and human disease. *Biochim Biophys Acta*. 2010;1797:113–128.
6. Fraser JA, Biousse V, Newman NJ. The neuro-ophthalmology of mitochondrial disease. *Surv Ophthalmol*. 2010;55:299–334.
7. Kang EY, Liu PK, Wen YT, et al. Role of oxidative stress in ocular diseases associated with retinal ganglion cells degeneration. *Antioxidants (Basel)*. 2021;10:1948.
8. Chan DC. Mitochondria: dynamic organelles in disease, aging, and development. *Cell*. 2006;125:1241–1252.
9. Carelli V, Ross-Cisneros FN, Sadun AA. Mitochondrial dysfunction as a cause of optic neuropathies. *Prog Retin Eye Res*. 2004;23:53–89.
10. Wallace DC, Singh G, Lott MT, et al. Mitochondrial DNA mutation associated with Leber's hereditary optic neuropathy. *Science*. 1988;242:1427–1430.
11. Alexander C, Votruba M, Pesch UE, et al. OPA1, encoding a dynamin-related GTPase, is mutated in autosomal dominant optic atrophy linked to chromosome 3q28. *Nat Genet*. 2000;26:211–215.
12. Cohn AC, Toomes C, Potter C, et al. Autosomal dominant optic atrophy: penetrance and expressivity in patients with *OPA1* mutations. *Am J Ophthalmol*. 2007;143:656–662.
13. Yu-Wai-Man P, Griffiths PG, Hudson G, Chinnery PF. Inherited mitochondrial optic neuropathies. *J Med Genet*. 2009;46:145–158.
14. Piro-Mégy C, Sarzi E, Tarrés-Solé A, et al. Dominant mutations in mtDNA maintenance gene SSBP1 cause optic atrophy and foveopathy. *J Clin Invest*. 2020;130:143–156.
15. Jurkute N, Leu C, Pogoda HM, et al. SSBP1 mutations in dominant optic atrophy with variable retinal degeneration. *Ann Neurol*. 2019;86:368–383.
16. Del Dotto V, Ullah F, Di Meo I, et al. SSBP1 mutations cause mtDNA depletion underlying a complex optic atrophy disorder. *J Clin Invest*. 2020;130:108–125.
17. Tiranti V, Rossi E, Ruiz-Carrillo A, et al. Chromosomal localization of mitochondrial transcription factor A (TCF6), single-stranded DNA-binding protein (SSBP), and endonuclease G (ENDOG), three human housekeeping genes involved in mitochondrial biogenesis. *Genomics*. 1995;25:559–564.
18. Huang J, Gong Z, Ghosal G, Chen J. SOSS complexes participate in the maintenance of genomic stability. *Mol Cell*. 2009;35:384–393.
19. Stone J, van Driel D, Valter K, Rees S, Provis J. The locations of mitochondria in mammalian photoreceptors: relation to retinal vasculature. *Brain Res*. 2008;1189:58–69.
20. Riordan-Eva P, Sanders MD, Govan GG, et al. The clinical features of Leber's hereditary optic neuropathy defined by the presence of a pathogenic mitochondrial DNA mutation. *Brain*. 1995;118:319–337.
21. Salomão SR, Berezovsky A, Andrade RE, et al. Visual electrophysiologic findings in patients from an extensive Brazilian family with Leber's hereditary optic neuropathy. *Doc Ophthalmol*. 2004;108:147–155.
22. Shibata K, Shibagaki Y, Nagai C, Iwata M. Visual evoked potentials and electroretinograms in an early stage of Leber's hereditary optic neuropathy. *J Neurol*. 1999;246:847–849.
23. Marmor MF, Fulton AB, Holder GE, et al. ISCEV standard for full-field clinical electroretinography (2008 update). *Doc Ophthalmol*. 2009;118:69–77.
24. Wang NK, Liu L, Chen HM, et al. Clinical presentations of X-linked retinoschisis in Taiwanese patients confirmed with genetic sequencing. *Mol Vis*. 2015;21:487–501.
25. Seo GH, Kim T, Choi IH, et al. Diagnostic yield and clinical utility of whole exome sequencing using an automated variant prioritization system, EVIDENCE. *Clin Genet*. 2020;98:562–570.
26. Cooper LL, Hansen RM, Darras BT, et al. Rod photoreceptor function in children with mitochondrial disorders. *Arch Ophthalmol*. 2002;120:1055–1062.
27. Lin CS, Sharpley MS, Fan W, et al. Mouse mtDNA mutant model of Leber hereditary optic neuropathy. *Proc Natl Acad Sci USA*. 2012;109:20065–20070.
28. Liu XT, Shen MX, Chen C, et al. Foveal pit morphological changes in asymptomatic carriers of the G11778A mutation with Leber's hereditary optic neuropathy. *Int J Ophthalmol*. 2020;13:766–772.
29. Gränse L, Bergstrand I, Thiselton D, et al. Electrophysiology and ocular blood flow in a family with dominant optic nerve atrophy and a mutation in the *OPA1* gene. *Ophthalmic Genet*. 2003;24:233–245.

Downloaded from iovs.arvojournals.org on 04/24/2024

30. Miyata K, Nakamura M, Kondo M, et al. Reduction of oscillatory potentials and photopic negative response in patients with autosomal dominant optic atrophy with OPA1 mutations. *Invest Ophthalmol Vis Sci*. 2007;48:820–824.
31. Reis A, Mateus C, Viegas T, et al. Physiological evidence for impairment in autosomal dominant optic atrophy at the pre-ganglion level. *Graefes Arch Clin Exp Ophthalmol*. 2013;251:221–234.
32. Cascavilla ML, Parisi V, Triolo G, et al. Retinal dysfunction characterizes subtypes of dominant optic atrophy. *Acta Ophthalmol*. 2018;96:e156–e163.
33. Heiduschka P, Schnichels S, Fuhrmann N, et al. Electrophysiological and histologic assessment of retinal ganglion cell fate in a mouse model for OPA1-associated autosomal dominant optic atrophy. *Invest Ophthalmol Vis Sci*. 2010;51:1424–1431.
34. Barboni P, Savini G, Parisi V, et al. Retinal nerve fiber layer thickness in dominant optic atrophy: measurements by optical coherence tomography and correlation with age. *Ophthalmology*. 2011;118:2076–2080.
35. Cesareo M, Ciuffoletti E, Martucci A, et al. Assessment of the retinal posterior pole in dominant optic atrophy by spectral-domain optical coherence tomography and microperimetry. *PLoS One*. 2017;12:e0174560.
36. Meschede IP, Ovenden NC, Seabra MC, et al. Symmetric arrangement of mitochondria:plasma membrane contacts between adjacent photoreceptor cells regulated by *Opa1*. *Proc Natl Acad Sci USA*. 2020;117:15684–15693.
37. Liu H, Prokosch V. Energy Metabolism in the inner retina in health and glaucoma. *Int J Mol Sci*. 2021;22:3689.
38. Narayan DS, Chidlow G, Wood JP, Casson RJ. Glucose metabolism in mammalian photoreceptor inner and outer segments. *Clin Exp Ophthalmol*. 2017;45:730–741.
39. Hurley JB, Lindsay KJ, Du J. Glucose, lactate, and shuttling of metabolites in vertebrate retinas. *J Neurosci Res*. 2015;93:1079–1092.
40. Carter-Dawson LD, LaVail MM. Rods and cones in the mouse retina. I. Structural analysis using light and electron microscopy. *J Comp Neurol*. 1979;188:245–262.
41. Perkins GA, Ellisman MH, Fox DA. Three-dimensional analysis of mouse rod and cone mitochondrial cristae architecture: bioenergetic and functional implications. *Mol Vis*. 2003;9:60–73.
42. Hoang QV, Linsenmeier RA, Chung CK, Curcio CA. Photoreceptor inner segments in monkey and human retina: mitochondrial density, optics, and regional variation. *Vis Neurosci*. 2002;19:395–407.
43. He J, Yamamoto M, Sumiyama K, et al. Two-photon AMPK and ATP imaging reveals the bias between rods and cones in glycolysis utility. *FASEB J*. 2021;35:e21880.
44. Bhatti JS, Bhatti GK, Reddy PH. Mitochondrial dysfunction and oxidative stress in metabolic disorders - a step towards mitochondria based therapeutic strategies. *Biochim Biophys Acta Mol Basis Dis*. 2017;1863:1066–1077.
45. Yildirim Z, Ucgun NI, Yildirim F. The role of oxidative stress and antioxidants in the pathogenesis of age-related macular degeneration. *Clinics (Sao Paulo)*. 2011;66:743–746.
46. Nita M, Grzybowski A. The role of the reactive oxygen species and oxidative stress in the pathomechanism of the age-related ocular diseases and other pathologies of the anterior and posterior eye segments in adults. *Oxid Med Cell Longev*. 2016;2016:3164734.
47. Qi X, Lewin AS, Hauswirth WW, Guy J. Optic neuropathy induced by reductions in mitochondrial superoxide dismutase. *Invest Ophthalmol Vis Sci*. 2003;44:1088–1096.
48. Kao S-H, Yen M-Y, Wang A-G, Yeh Y-L, Lin A-L. Changes in mitochondrial morphology and bioenergetics in human lymphoblastoid cells with four novel *OPA1* mutations. *Invest Ophthalmol Vis Sci*. 2015;56:2269–2278.
49. Wallace DC, Lott MT. Leber hereditary optic neuropathy: exemplar of an mtDNA disease. *Handb Exp Pharmacol*. 2017;240:339–376.
50. Chun BY, Rizzo JFI. Dominant optic atrophy: updates on the pathophysiology and clinical manifestations of the optic atrophy 1 mutation. *Curr Opin Ophthalmol*. 2016;27:475–480.
51. Kang JS, Tian JH, Pan PY, et al. Docking of axonal mitochondria by syntaphilin controls their mobility and affects short-term facilitation. *Cell*. 2008;132:137–148.
52. Ito YA, Di Polo A. Mitochondrial dynamics, transport, and quality control: a bottleneck for retinal ganglion cell viability in optic neuropathies. *Mitochondrion*. 2017;36:186–192.
53. Bros H, Millward JM, Paul F, Niesner R, Infante-Duarte C. Oxidative damage to mitochondria at the nodes of Ranvier precedes axon degeneration in ex vivo transected axons. *Exp Neurol*. 2014;261:127–135.
54. Coussa RG, Merat P, Levin LA. Propagation and selectivity of axonal loss in Leber hereditary optic neuropathy. *Sci Rep*. 2019;9:6720.
55. Meunier I, Bocquet B, Defoort-Dhellemmes S, et al. Characterization of SSBP1-related optic atrophy and foveopathy. *Sci Rep*. 2021;11:18703.
56. Veitia RA, Caburet S, Birchler JA. Mechanisms of Mendelian dominance. *Clin Genet*. 2018;93:419–428.
57. Gustafson MA, Sullivan ED, Copeland WC. Consequences of compromised mitochondrial genome integrity. *DNA Repair (Amst)*. 2020;93:102916.

Investigative Ophthalmology & Visual Science

Downloaded from iovs.arvojournals.org on 04/24/2024